JOURNAL OF OPTOELECTRONICS AND ADVANCED MATERIALS Vol. 9, No. 5, May 2007, p. 1395 - 1398

Sol gel porous ZnO thin films for gas sensing applications

V. MUSAT*, E. FORTUNATO[a], F. BRAZ FERNANDES[a], R. JORGE CORDEIRO SILVA[a]
Department of Metals and Materials Science, "Dunărea de Jos" University of Galati, Romania
[a]New University of Lisbon, Material Science Department, CENIMAT, Portugal

Undoped and doped ZnO porous thin films are very interesting gas sensitive materials. The paper presents the properties of porous zinc oxide thin films deposed on soda-lime-glass substrate via dip-coating technique, using zinc acetate dihidrate, ethanol and monoethanol amine as raw materials. The effect of withdrawal speed on the crystalline structure, morphology, optical, electrical and gas sensing properties of the thin films has been investigated using XRD, AFM, optical transmittance and typical photoreduction-ozone reoxidation cycles.

(Received November 14, 2006; accepted April 12, 2007)

Keywords: Gas-sensor, Microstructure, Zinc oxide, Thin film, Sol-gel

1. Introduction

ZnO is an important low cost multifunctional material with actual and potential applications in numerous fields as displays, solar cells, electrochromic devices, surface acoustic wave devices (SAW) for communication, transistors and very efficient light-emitting materials for short wavelength optoelectronic devices, UV and blue LEDs and lasers.

Undoped and doped ZnO thin films with porous structure are very interesting gas sensitive materials. As gas sensor material, ZnO can be used to detect reducing gases (CO and H_2) [1-3], O_2 [4], O_3 [5-7] or humidity [8]. Very recently, nanocrystalline ZnO gas sensors have attracted more interest due to its better properties of detecting pollutants, toxic gases, alcohols and food freshness, especially fish freshness [9], or as gas-sensing films integrated on one chip to make an "electronic nose" [10-11].

The sol-gel technique offers the greatest possibility of preparing low cost small as well as large-area functional oxide thin films due to controllability of film composition and microstructure [12-16]. It is well know that the sensing mechanism of semiconducting oxide gas sensors is based on the surface reaction and a high surface-volume ratio. The grain size and the porosity of sensing film are the most important factors for high sensitivity and short response time sensors. When dip-coating sol-gel technique is used, the withdrawal speed is the most important processing parameter affecting the porosity of the sensing films.

This paper presents the properties of zinc oxide thin films deposed on soda-lime-glass substrate, via dip-coating technique. The effect of withdrawal speed on the crystalline structure, morphology, optical, electrical and gas sensing properties of the thin films has been investigated using XRD, AFM, optical transmittance and typical photoreduction-ozone reoxidation cycles.

2. Experimental

2.1. Films preparation

The sol was prepared by dissolution of zinc acetate dihydrate (99.5%) in ethanol and monoethanol amine (MEA). The molar ratio of MEA to zinc acetate was 1.0 and the concentration of zinc acetate was 0.5M. The thin films were deposed on soda-lime-glass substrates by dip-coating technique with different withdrawal speed in the range 10-20 cm/min, at room temperature (RT) and room humidity (RH) conditions. After each layer deposition, the gel film was stabilized by pre-heating in air for 10 minutes at 400 ^oC. The procedure was repeated 4 times. The stabilized films were then crystallized by post-heating 1 hour in air at 500 ^oC. Final thickness of about 120, 160 and 195 nm was obtained for the crystallyzed films deposed at 10, 15 and 20 cm/min, respectively.

2.2. Films characterization

The thickness of the thin films was measured using a Sloan Dektak 3D surface profilometer.

The XRD patterns of the samples were recorded at room temperature using a Rigaku diffractometer (model DMAX-IIIC), with CuKα radiation.

The morphology on the surface of the films was analyzed using an AFM microscope. Tapping mode AFM experiments were performed in a Nanoscope IIIa Multimode AFM microscope (Digital Instruments, Veeco). Commercial etched silicon tips with typical resonance frequency of ca. 300 Hz (RTESP, Veeco) have been used as AFM probes.

The electrical resistivity of the films was measured in dark, using a KEITHLEY 617 Model Programmable Electrometer.

The optical transmittance was measured using a UV-VIS-NIR double beam spectrophotometer (Shimadzu, UV-3100 PC) in the wavelength range 200 to 2500 nm. From the optical measurements, the *optical energy gap*, E_{gap}, was calculated assuming a direct transition between the edges of the valence and the conduction band, for which the variation in the absorption coefficient α with photon energy hν is given by the equation:

$$(\alpha h\nu)^2 = B(h\nu - E_{gap}) \quad (1)$$

By plotting $(\alpha h\nu)^2$ versus hν, and extrapolating the linear region of the resulting curves, E_{gap} was obtained.

2.3. Sensing test

The gas (ozone) sensing properties were investigated by electrical measurements at room temperature, which were carried out in a special chamber presented elsewhere [5, 6]. The conductivity of ZnO film decreases when it is exposed to an ozone atmosphere. Because the films are resistive, first, its conductivity was increased by photoreduction, when the films were directly irradiated in vacuum by the UV light of a mercury pencil lamp with an average intensity of 4 mW/cm^2 for 20 min. After that, the chamber was backfilled with oxygen at a presure of 600 Torr and an UV lamp was used to produce ozone (the films is shielded from the lamp). The films were mainend for 40 min in this ozone atmosphere, when the re-oxidation of zinc oxide crystallites results in a decrease of film conductivity. An electric field of 50 V/cm was applied to the film sample and the electrical curent was measured.

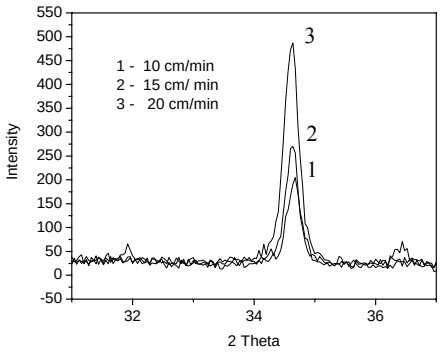

Fig. 1. XRD patterns of ZnO thin films deposed with different withrawal speed.

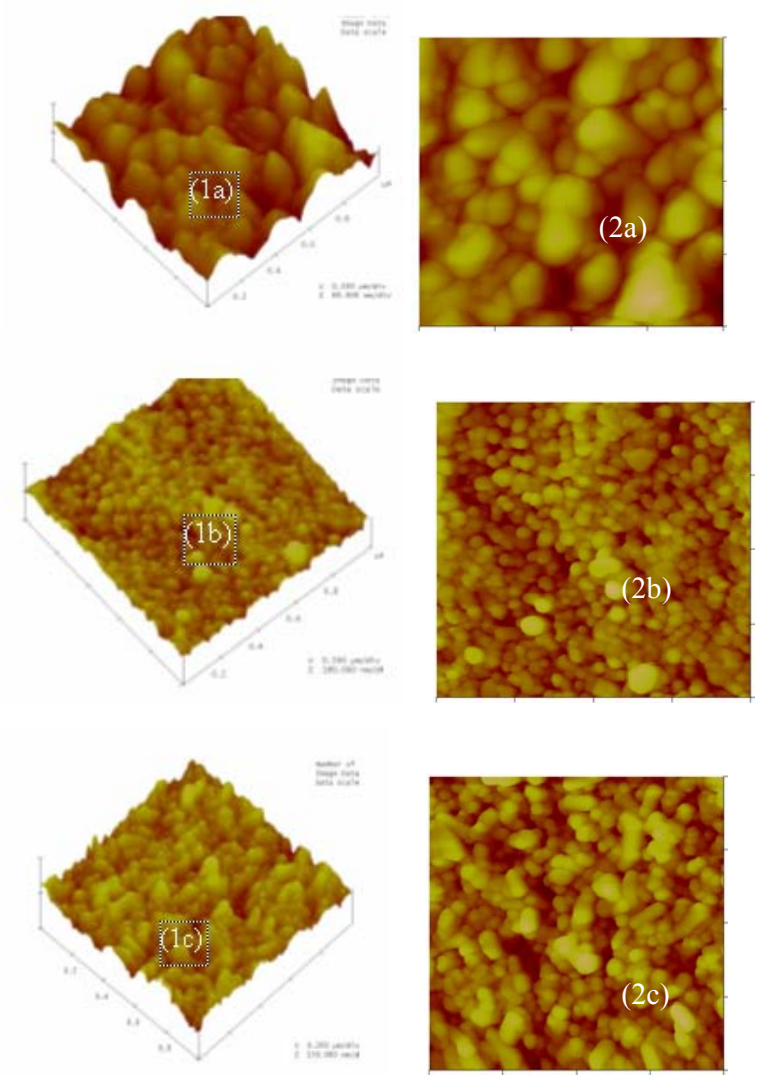

Fig. 2. AFM surface images, 3D (1) and topography (2), of ZnO thin films deposed with different withrawal speed: 10 cm/min (a), 15 cm/min (b) and 20 cm/min (c). The shown area is 1 × 1 μm^2.

3. Results and discussions

Figs. 1 and 2-3 show, respectively, the XRD patterns and AFM images of the films post-heat treated one hour at 500 ^{o}C in air. The XRD patters of the films show a (002) peack, indicating a high preferential c-axis orientated wurtzite type crystalline structure with grains perpendicular to the substrate surface. AFM images (Fig. 2) confirm this orientation and show porous, crack free films morphology with average grain size and pores size depending on the withdrawal speed. The grain size decreased when the withdrawal speed increased from 10 to 15 cm/min and then slightly increased when the withdrawal speed increased to 20 cm/min. The films porosity increased when the withdrawal speed increased. The film deposed at 20 cm/min presents two types of pores: roundish mesopores less than 50 nm diameter and macropores higher than 50 nm diameters; a macropore is built up around a mesopore (Fig. 3). One can notice a very weak grains agglomeration tendency when the withdrawal speed increased. The surface roughness mean square (rms) of the films estimated from AFM measurements decrease from about 60 to 50 nm, when the withdrawal speed increases from 10 cm/min to 20 cm/min, respectively. These roughness values are found to be large.

Fig. 3. AFM surface image of ZnO thin films deposed with 20 cm/min (Detail from figure 2c). The shown area is 0.5 x 0.5 μm^2. The z-range of the images is 75 nm.

Electrical resistivity values between 7×10^8 and 9×10^9 Ωcm have been obtained for ZnO thin film annealed in air. The electrical resistivity depends on the films porosity, increasing with the porosity increasing.

Fig. 4 show typical photoreduction-oxidation cycles of the films. The photoreduction-reoxidation behavior is quasi-reversible during cyclic treatments. The shape of the cycles depends on the porosity and the grain size of the polycrystalline films. From Fig. 4, one can notice that the more porous films deposed at 20 cm/min showed beter sensing response than the film deposed at 10 cm/min.

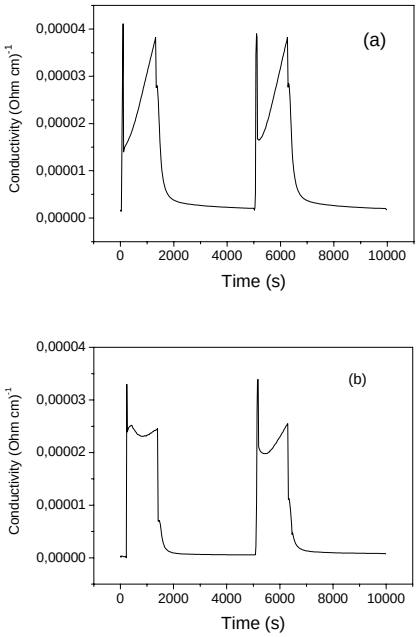

Fig. 4. Typical photoreduction - oxidation cycles (room temperature) of ZnO thin films deposed with 10 cm/min (a) and 20 cm/min (b).

The optical transmittance of thin films within the visible and the near infrared region was higher than 70% (Fig. 5). Surface morphology affects the optical properties of the film. Increasing porosity and decreasing grain size at higher withdrawal speed deposition, led to different variation of optical transmittance in the visible range: a decrease in 400-600 nm range and an increase in the 600-800 nm range (Fig. 5). The decrease in transmittance may be due to increasing optical scattering caused by increasing grain boundary density in the more porous and smaler grain films deposed with higher withdrawal speed. The optical transmittance data have been used for the calculation of direct optical energy gap (Fig. 6), according to the equation (1). The obtained E_{gap} values varied between 3,47 and 3,59 eV when the withdrawal speed varied between 10 cm/min and 20 cm/min.

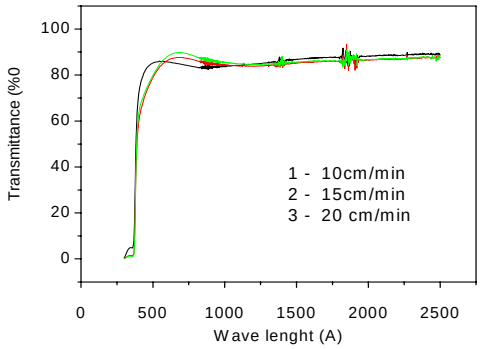

Fig. 5. Optical transmittance spectra of ZnO thin films deposed with different withrawal speed.

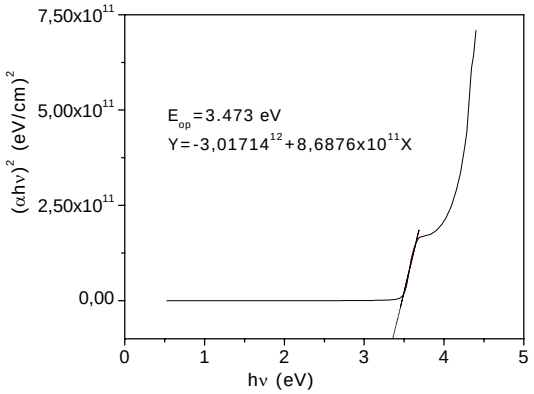

Fig. 6. The plot $(\alpha h\nu)^2$ vs. hν and the calculation of the optical energy gap (E_{gap}) of ZnO thin films deposed with 10 cm/min.

4. Conclusions

Transparent porous ZnO thin films on soda-lime-glass substrate were prepared by dip-coating technique, using zinc acetate dihidrate, ethanol and monoethanol amine as raw materials. The withdrawal speed is significantly affecting the crystalline structure, morphology, optical and gas-sensing properties of porous ZnO thin films.

ZnO thin films are polycrystalline with high preferred c-axis orientated hexagonal structure. The grain size and the pores size modified when the withdrawal speed increased.

The investigated films reveal reversible room temperature change in electrical resistance during UV irradiation followed by re-oxidation in ozone atmosphere. The shape of the photoreduction - reoxidation cycles depends on the porosity and the grain size of the polycrystalline films. The gas sensing response improved when the porosity increased and the grain size decreased.

The films show optical transmittance between 70 and 90% within the VIS and NIR wavelength region.

Acknowledgments

This work was supported by NATO Expert Visiting PDD(CP)-CBP.EAP.EV 982079 /2005 Grant.

References

[1] H.-Y. Bae, G.-M Choi, Sensors and Actuators. Chemical **B55**, 47-54 (1999).
[2] S. Roy, S. Basu, Bull. Mater. Sci. **25**, 513-515 (2002).
[3] S. Shukla, S. Patil, S.C. Kuiry, Z. Rahman, T. Du, Chemical B **96**, 343-353 (2003).
[4] A. Trinchi, Y.X. Li, W. Wlodarski, S. Kaciulis, L. Pandolfi, S.P. Russo, J. Duplessis, S. Viticoli, Physical A **108**, 263-270 (2003).
[5] M. Bender, E. Gagaoudakis, E. Douloufakis, N. Natsakou, N. Katsarakis, V. Cimalla, G. Kiriakidis, E. Fortunato, P. Nunes, A. Marques, R. Martins, Thin Solid Films **418**, 45-50 (2002).
[6] G. Kiriakidis, N. Katsarakis, M. Bender, N. Gagaoudachis, V. Cimalla, Mater. Phys. Mech. **1**, 83-86 (2000).
[7] N. Katsarakis, M. Bender, V. Cimalla, E. Gagaoudakis, G. Kiriakidis, Sensors and Actuators, Chemical **B96**, 76-81 (2003).
[8] W. P. Tai, J. H. Oh, J. Mat. Sci. **13**, 391-394 (2002).
[9] H. Tang, M. Yan, X. Ma, H. Zhang, M. Wang, D. Yang, et al, Sensors and Actuators, Chemical B113, 324-328 (2006).
[10] W. Shen, Y. Zhao, C. Zhang, Thin Solid Films **483**, 382-387 (2005).
[11] Q. Zhang, C. Xie, S. Zhang, A. Wang, B. Zhu, L. Wang, Z. Yang, Sensors and Actuators, Chemical, **B110**, 370-376 (2005).
[12] M. Zaharescu, M. Crisan, L. Predoana, M. Gartner, D. Cristea, S. Degeratu, E. Manea, J. Sol-Gel Sci. Tech. **32**, 173 –175 (2004).
[13] M. Zaharescu, M. Crisan, I. Musevic, J. Sol-Gel Sci. Tech. 1**3**, 769-773 (1998).
[14] Y. S. Kim, W.-P. Tai, S.-J. Shu, Thin Solid Films, **491**, 153-160 (2005).
[15] C.-Y. Zhang, X.-M. Li, X. Zhang, W.-D. Yu, J.-L. Zhao, J. Cryst. Growth, **290**, 67-72 (2006).
[16] H. Li, J. Wang, H. Liu, C. Yang, H. Xu, X. Li, H. Cui, Vacuum **77**, 57-62 (2004).

*Corresponding author: viorica.musat@ugal.ro